Comparison of elemental and black carbon measurements during normal and heavy haze periods: implications for research

Guorui Zhi · Yingjun Chen · Zhigang Xue ·
Fan Meng · Jing Cai · Guoying Sheng · Jiamo Fu

Abstract Studies specifically addressing the elemental carbon (EC)/black carbon (BC) relationship during the transition from clean-normal (CN) air quality to heavy haze (HH) are rare but have important health and climate implications. The present study, in which EC levels are measured using a thermal-optical method and BC levels are measured using an optical method (aethalometer), provides a preliminary insight into this issue. The average daily EC concentration was 3.08 ± 1.10 μg/m^3 during the CN stage but climbed to 11.77 ± 2.01 μg/m^3 during the HH stage. More importantly, the BC/EC ratio averaged 0.92 ± 0.14 during the CN state and increased to 1.88 ± 0.30 during the HH state. This significant increase in BC/EC ratio has been confirmed to result partially from an increase in the in situ light absorption efficiency (σ_{ap}) due to an enhanced internal mixing of the EC with other species. However, the exact enhancement of σ_{ap} was unavailable because our monitoring scheme could not acquire the in situ absorption (b_{ap}) essential for σ_{ap} calculation. This reveals a need to perform simultaneous measurement of EC and b_{ap} over a time period that includes both the CN and HH stages. In addition, the sensitivity of EC to both anthropogenic emissions and HH conditions implies a need to systematically study how to include *EC complex* (EC concentration, OC/EC ratio, and σ_{ap}) as an indicator in air quality observations, in alert systems that assess air quality, and in the governance of emissions and human behaviors.

G. Zhi · Z. Xue · F. Meng · J. Cai
State Key Laboratory of Environmental Criteria
and Risk Assessment, Chinese Research Academy
of Environmental Sciences, Beijing 100012, China

Y. Chen (✉)
Key Laboratory of Coastal Zone Environmental Processes
and Ecological, Yantai Institute of Coastal Zone Research,
Chinese Academy of Sciences (CAS), 17 Chunhui Road,
Laishan District, Yantai, Shandong 264003, China
e-mail: yjchen@yic.ac.cn

J. Cai · G. Sheng · J. Fu
State Key Laboratory of Organic Geochemistry,
Guangzhou Institute of Geochemistry,
CAS, Guangzhou 510640, China

Introduction

The past three decades have seen increasing interest in black carbon (BC) and elemental carbon (EC), both of which originate from the incomplete combustion of carbonaceous combustibles, due to their strong light-absorbing properties and their possible health effects (Johnson and Huntzicker 1979; Wolff 1981; Turco et al. 1983; Molnar et al. 1999; Jacobson 2000, 2001; Ramanathan and Carmichael 2008; Allen et al. 2012). EC represents thermally refractory carbon with a graphitic structure, whereas BC is commonly used to define the extent to which an aerosol sample exhibits light-absorbing properties (Salako et al. 2012; Gray and Cass 1998; Huntzicker et al. 1982; Watson et al. 2005).

The quantification of EC and BC is dependent on the method employed. EC is often determined using thermal–optical protocols, such as National Institute of Occupational Safety and Health Method 5040 with correction by thermal–optical transmission (NIOSH/TOT) (Birch 1998, 2002; Birch and Cary 1996; Stone et al. 2010; Kaul et al. 2011) or the Interagency Monitoring of Protected Visual Environments with correction by thermal–optical reflectance (IMPROVE/TOR) (Chow et al. 1993, 2007; Pavuluri et al. 2011). BC cannot be measured directly but must be inferred from the particle light absorption (b_{ap}) through a conversion factor that is used to translate b_{ap} to the BC mass concentration (Chow et al. 2009; Biswas et al. 2003). According to the literature, both EC and BC are considered to assume a graphitic structure and are therefore thermally refractory and light-absorbing in nature (Bond and Bergstrom 2006; Salako et al. 2012; Conny et al. 2003; Turpin et al. 1990). It seems that both EC and BC describe nearly the same fraction of carbonaceous aerosols; however, according to traditional practice, their values are dependent on specified determination methods which focus on different properties, e.g., thermal stability or light absorption (Birch 1998; Chow et al. 1993; Hansen et al. 1984). This practice introduces the potential for disagreement between EC and BC measurements due to method-involved biases (Jeong et al. 2004; Lavanchy et al. 1999; Li et al. 2006; Salako et al. 2012).

It is reasonable to think that once the measurement methods for EC and BC have been chosen, the measured BC/EC ratio ought to be somewhat constant for identical carbonaceous aerosols, but these values may be inconsistent for different carbonaceous aerosols with different optical properties. This assumption allows for a means of evaluating the optical characteristics and changes in carbonaceous aerosols under significant air pollution, such as heavy urban haze.

Following rapid industrialization, urbanization, and economic development, the expanding energy consumption in China has not only contributed more greenhouse gases to the atmosphere but has also decreased the levels of solar radiation and horizontal visibility since the 1980s (Chang et al. 2009; Che et al. 2007). When visibility drops below 10 km, the conditions are considered to be a haze event (Deng et al. 2008; Wu et al. 2005). Because atmospheric aerosol plays an important role in global and regional energy budgets, the recently increased incidence of heavy urban haze in China is indicative of the growing impact of urban aerosols on both air quality and climate (Engling and Gelencsér 2010; Ramanathan and Feng 2009; Seinfeld and Pandis 1998). Although a number of comparisons of simultaneous EC and BC measurements for urban or non-urban ambient aerosols have been reported (Lavanchy et al. 1999; Li et al. 2006; Salako et al. 2012; Jeong et al. 2004; Cyrys et al. 2003; Nordmann et al. 2009), studies specifically characterizing the EC/BC relationship during a transition from normal air quality to heavy haze are rare.

This study, in which EC is measured using a thermal-optical method and BC is measured using an aethalometer, aims to address the changes in the BC/EC relationship that arise as the air quality transitions from a normal state to heavy haze conditions and will promote an enhanced understanding of the effects of changing aerosols on both air quality and climate, with important implications for future research.

Materials and methods

Parallel PM$_{2.5}$ inlets for an aethalometer and a MiniVol sampler

The experimental monitoring was performed in Shanghai, a coastal megacity in China with a population of approximately 18 million and a land area of approximately 6,340 km^2. Heavy haze (HH) frequently occurs during late autumn and winter due to high anthropogenic emissions coupled with stagnant meteorological conditions. According to publicly available data from the Shanghai Environmental Monitoring Center, PM$_{10}$ usually peaks in November or December (http://www.envir.gov.cn/). Our monitoring was performed during this period to investigate the distinctive changes in aerosol optics that occur under HH conditions.

Sampling was performed at the Yanchang campus of Shanghai University in the Zhabei District from 10:00 a.m. on Nov. 14 to midnight on Nov. 27. This site is composed of mixed residential, traffic, and commercial environments in an urban area (Feng et al. 2009). Two parallel PM$_{2.5}$ inlets (≤2.5 μm in particle diameter) were deployed side-by-side on the rooftop of the College of Chemical and Environmental Science building at Shanghai University. One of the inlets was connected to a MiniVol sampler (AirMetric), whereas the other was connected to an aethalometer (AE42, Magee Scientific). The flow rate for both inlets was set

at 5 L/min to ensure the accuracy both of the PM$_{2.5}$ size cut and of the designed comparison between the aethalometer-measured BC and the Sunset carbon analyzer-measured EC.

Determination of PM$_{2.5}$, EC, and organic carbon (OC)

Each quartz filter (Millipore, 47-mm diameter) used in the MiniVol sampler was weighed using an electronic balance (Sartorius, 0.01 mg, Germany) at a temperature of 25 °C and a relative humidity of 50 % before and after sampling. The PM$_{2.5}$ concentration was calculated according to the collected particle mass and the corresponding air volume. A thermal/optical transmission carbon analyzer (Sunset Laboratory Inc.) was employed to divide the filter-loaded particulate carbon into OC and EC (Birch and Cary 1996). The temperature protocol was similar to NIOSH Method 5040 and has been described in our previous publications (Zhi et al. 2008, 2009, 2011).

Determination of BC

As the principle behind using an aethalometer for BC determination has been described elsewhere (Hansen et al. 1984; Jeong et al. 2004; Lavanchy et al. 1999), only a brief description will be provided here. The aethalometer samples ambient air through a quartz filter tape at a flow rate of 5 L/min. The attenuation (ATN) at 880 nm through the particle-laden section of a filter spot is measured every 5 min. BC concentration is estimated by conversion of corresponding ATN through a designated conversion factor, $\sigma_{ATN\text{-}d}$:

$$\text{BC} = \text{ATN} \Big/ \sigma_{ATN-d}$$

It is imaginable that if the actual attenuation efficiency ($\sigma_{ATN\text{-}a}$) diverges from the $\sigma_{ATN\text{-}d}$ used in the aethalometer, reported BC values will also diverge from EC values.

Identification of HH days and clean-normal (CN) days

An unambiguous method for distinguishing between HH days and CN days is a prerequisite for this study. A haze day is assumed when all of the following conditions are met: a daily mean visibility <10 km, a daily mean relative humidity <90 %, and little or no precipitation (Deng et al. 2008; Wu et al. 2005). In contrast, a CN day is assigned when the hourly visibility is always or usually higher than 10 km. Because we are more interested in the characteristics of HH conditions, we identify an HH day when the hourly visibility is usually <5 km. According to the above criteria, our 2-week monitoring program, from 10:00 a m. on Nov. 14 to midnight on Nov. 27, can generally be divided into two stages: a CN stage during the first week (Nov. 14–20, excluding Nov. 18) and a HH stage during the second week (Nov. 21–27). Most of the data for the first week indicated high visibility levels (at least 10 km), whereas in the second week, the visibility decreased to 2.7± 0.5 km on average, indicating the presence of intense haze (Fig. 1a, b).

Although the information for Nov. 18 is given in all of the related figures or table in this study to provide continuity for the time series, this information was always excluded from the relevant calculations for the CN week because the hourly visibility repeatedly fell below 10 km on that day (Fig. 1a). As a result, there are only 6 days in the CN week. Furthermore, because the hourly visibility for Nov. 18 was generally higher than 5 km, this day was not categorized within the HH period either. In addition, although the visibility dropped sharply after 10:00 p m. on Nov. 20, our sampling on that day ended at 9:00 p m., enabling the data observed on Nov. 20 to purely represent the CN state.

Additional parameters were used to corroborate the CN and HH designations. During the CN week, the average PM$_{2.5}$, SO$_2$, and NO$_2$ levels were 43±16, 41± 11, and 39±6 μg/m^3, respectively, whereas during the HH week, the average PM$_{2.5}$, SO$_2$, and NO$_2$ levels rose to 265±69, 126±26, and 114±20 μg/m^3, respectively, corresponding to 6.2-, 3.1-, and 3.9-fold increases relative to the values for the CN week (Fig. 2). Moreover, the wind speed dropped from 4.6±2.0 m/s during the first week to 1.1±1.4 m/s during the second week, suggesting that the local atmosphere was extremely stagnant horizontally during the HH stage (Fig. 1a). More importantly, the vertical temperature profile during the HH week was conducive to the formation of urban haze. Figure 3 displays two Skew-T charts for Nov. 25 at 0:00 and 12:00, derived from a sounding at the Shanghai station (No. 58362) (http://weather.uwyo.edu). Obviously, a typical inversion in the lower atmosphere occurred and suppressed the upward dispersal of air pollutants, leading to HH conditions throughout the day. A careful review of the website records over the entire 2-week experimental duration
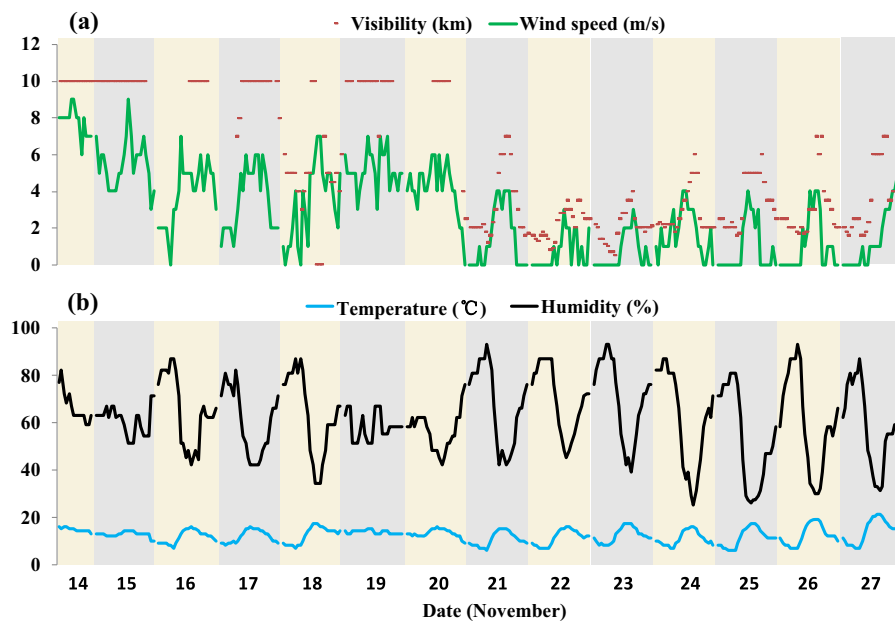
Fig. 1 Temporal variations in the visibility, wind speed, temperature, and humidity during the observation period. Data were obtained from Weather Underground (http://www.wunderground.com); some of the observation data (particularly for the visibility on NC days) were unavailable due to incomplete availability in the web data set. Visibilities equal to or greater than 10 km are given as 10 km in the web data and are accordingly presented in this figure

confirmed that this temperature inversion occurred every day during the HH week, in sharp contrast to the first week, during which no temperature inversions were observed, implying the primary role of meteorological conditions in the development of heavy urban haze.
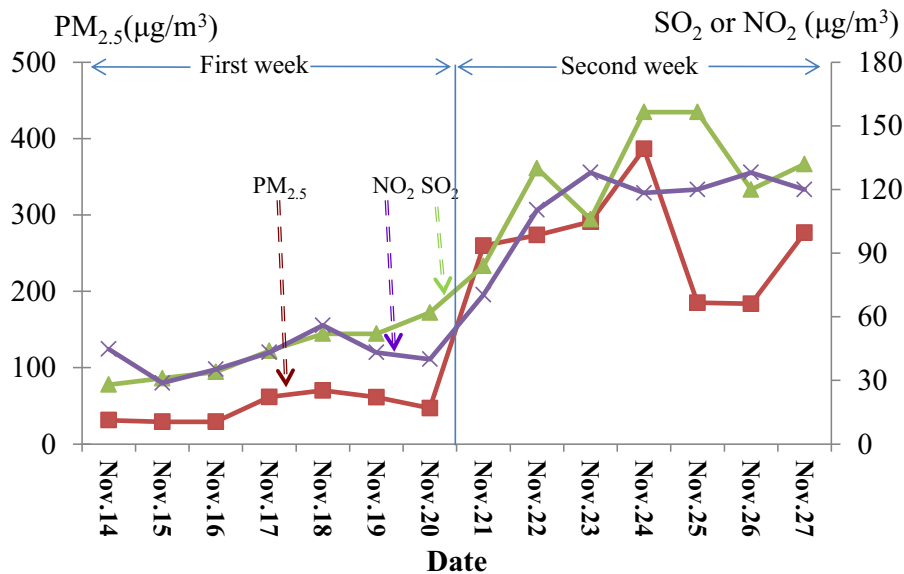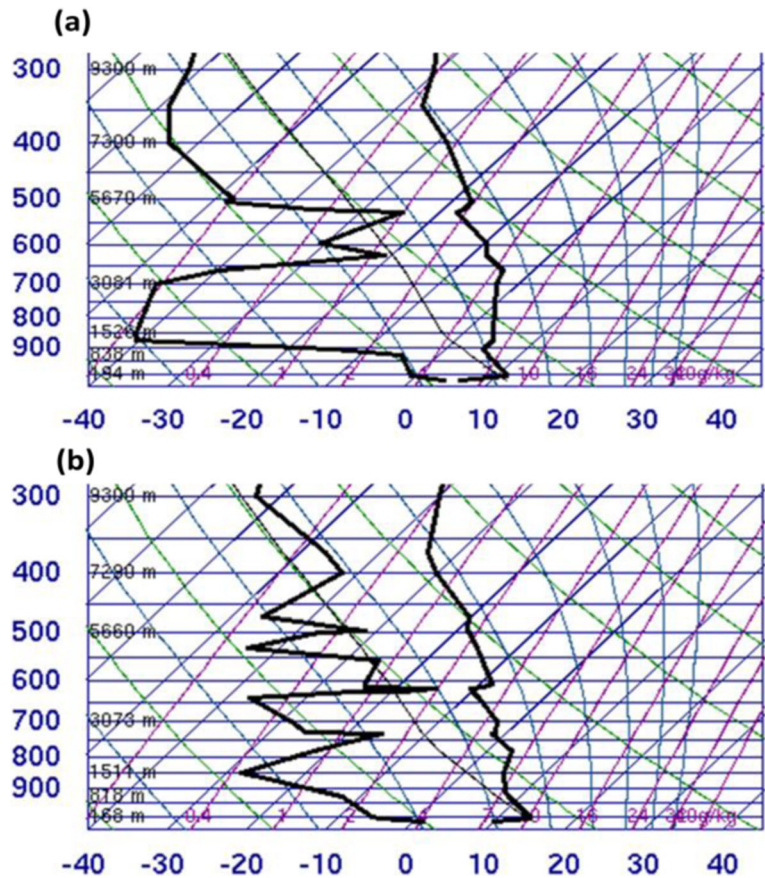

Fig. 2 Daily variations in PM$_{2.5}$, SO$_2$, and NO$_2$ during the observation period. The atmospheric concentrations of SO$_2$ and NO$_2$ are derived from the Air Pollution Indexes (APIs) listed on the website of the Shanghai Environmental Monitoring Center (http://www.semc.com.cn). The PM$_{2.5}$ concentrations were measured in this study

Results and discussion

Variation of EC and BC concentrations for CN and HH periods

Daily EC concentrations were calculated according to the thermal–optical speciation of on-filter carbon and the corresponding air volume; daily BC concentrations were obtained by averaging all of the 5-min readings for each calendar day (see Table 1). Figure 4 shows the variation in EC and BC concentrations over the entire observation period, which displays a noticeable contrast between the CN and HH weeks. During the CN week, the daily EC concentration was 3.08 ± 1.10 μg/m^3 (mean $\pm$s), whereas during the HH week, the daily EC concentration climbed to 11.77 ± 2.01 μg/m^3, which indicates a nearly fourfold increase relative to values obtained during the CN week. This result may be due to the stagnant meteorological conditions that led to the buildup of mainly local pollutants including ambient EC (Tan et al. 2009).
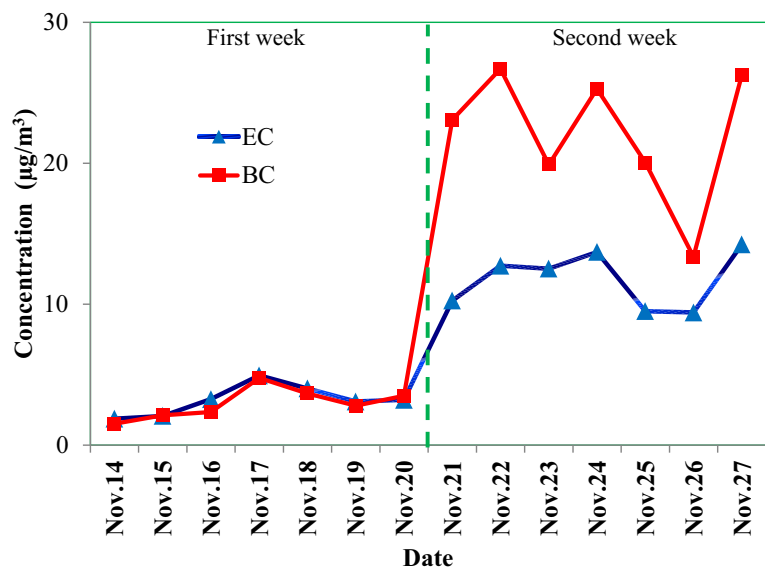
In addition, the BC/EC relationship during the CN week differed from that of the HH week. As shown in Fig. 4, during the CN week, the variations in BC was similar to those of EC, and the average BC/EC ratio was 0.92 ± 0.14, which is very close to 1. This result conforms to the general viewpoint that EC is a major contributor to ambient aerosol light absorption and explains why EC is often used interchangeably with BC when the aerosol effect on climate is considered, when an aethalometer needs calibrating, or when BC emission inventories are developed (Conny et al. 2003; Vignati et al. 2010; Petzold et al. 1997). However, the trends shifted abruptly during the HH week, with the BC levels consistently higher than the corresponding EC levels. A comparison of BC and EC concentrations demonstrates that the BC/EC ratio increased to 1.88 ± 0.30 at the initiation of HH conditions on Nov. 21, more than doubling that for the CN period. Analysis using SPSS software demonstrated a significant difference in the BC/EC ratios between the HH and CN stages. The mechanism behind this change and the possible implications of this finding merit further study.

Table 1 Measured results for daily concentrations of $PM_{2.5}$, EC, OC, and BC ($\mu g/m^3$)

Air conditions	Date	$PM_{2.5}$	EC	OC	BC
Clean normal (CN)	Nov. 14	31.21	1.87	5.02	1.52
	Nov. 15	29.17	2.07	5.68	2.12
	Nov. 16	29.17	3.26	8.24	2.34
	Nov. 17	61.64	4.95	10.78	4.77
	Nov. 18	70.18	4.02	11.78	3.67
	Nov. 19	61.32	3.10	8.55	2.80
	Nov. 20	47.11	3.21	8.47	3.49
	Means	43.27	3.08	7.79	2.84
		15.63	1.10	2.11	1.15
Heavy haze (HH)	Nov. 21	259.86	10.25	59.17	23.09
	Nov. 22	273.61	12.73	60.46	26.70
	Nov. 23	291.20	12.52	62.24	19.90
	Nov. 24	386.43	13.70	85.91	25.28
	Nov. 25	185.00	9.50	51.02	20.05
	Nov. 26	183.64	9.41	48.47	13.36
	Nov. 27	276.71	14.24	75.88	26.27
	Means	265.21	11.77	63.31	22.09
		69.15	2.01	13.33	4.75

Exploratory probe of the BC/EC divergence in the HH period

The similarity in BC and EC concentrations during the CN week, combined with the divergence during the HH week, implies a change in the optical properties of atmospheric aerosols for the two conditions. This change is likely due to differences in factors such as chemical composition, mixing state, and relative humidity (Salako et al. 2012; Jeong et al. 2004; Andreae and Gelencsér 2006; Redemann et al. 2001).

In this study, an increased formation of secondary OC aerosols (SOCs) during the HH period was clearly observed, which altered the chemical composition as well as the physical structure. SOC is typically estimated from the OC/EC ratio (Castro et al. 1999; Turpin and Huntzicker 1995):

$$SOC = TOC - EC \times \left(OC \Big/ EC \right)_{primary}$$

where $(OC/EC)_{primary}$ is the ratio for primary source emissions and is usually represented by the lowest OC/EC ratio throughout the observation period. When the observed OC/EC ratio exceeds $(OC/EC)_{primary}$, SOCs are considered to have been formed. As shown in Fig. 5, the SOC fraction significantly increased from 0.15 ± 0.08 in the CN week to 0.59 ± 0.04 in the HH week, indicating that secondary organic aerosols became the largest fraction of the total organic aerosols during the HH period. Similar changes in the secondary aerosol fraction with the formation of compounds such as sulfate, nitrate, and ammonium have also been reported in Shanghai and other Chinese cities under HH conditions, suggesting that increased SOC formation is a common consequence of heavy urban haze (Sun et al. 2006; Tan et al. 2009; Yang et al. 2011).
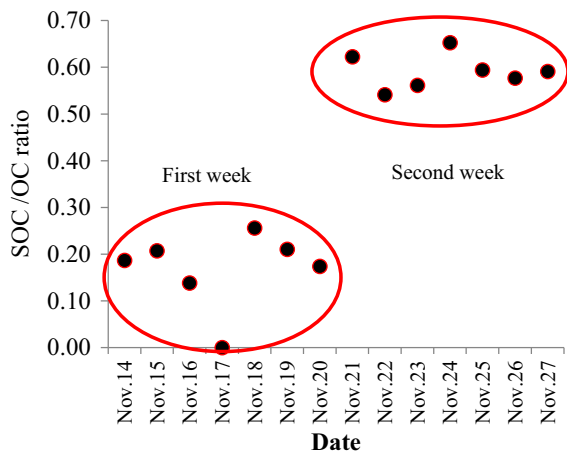
Fig. 4 Temporal variations in EC and BC

Fig. 5 Changes in the ratio of secondary OC to total OC (SOC/OC). The OC/EC ratio for Nov. 17 is the lowest among the observation period and is regarded as the reference scenario (SOC/OC=0)

Particles are considered "aged" when a high percentage of secondary species is formed (Liu et al. 2003; Yang et al. 2011); aged carbonaceous aerosols become more internally mixed in, e.g., a shell-core structure with other species. For example, Yang et al. (2011) observed that most submicron carbonaceous aerosols were internally mixed with ammonium nitrate and secondary organic compounds during the HH episode of Shanghai winter. Both theory and practice have demonstrated that the absorption efficiency (σ_{ap}) of EC in the internal mixing pattern is much higher than that in the external mixing pattern (Jacobson 2001; Ramanathan and Carmichael 2008; Bond et al. 2013). Apparently, this trend will partially (rather than completely) account for the higher BC levels observed under HH conditions in comparison to EC unambiguously.

Other changes in the aerosol composition such as dust or brown carbon may also bias the filter-based measurements of light absorption (Andreae and Gelencsér 2006; Li et al. 2006). However, the stagnancy of HH weather tends to confine the monitored urban aerosols to mainly their source location (Tan et al. 2009), and therefore, the contribution of imported dust under HH conditions should not be greater than that under CN conditions. In other words, dust is unlikely to have caused the aforementioned CN-to-HH elevation of σ_{ap}. Regarding brown carbon, a wavelength of 880 nm was used in the aethalometer for BC quantification, at which brown carbon is theoretically almost invisible (Andreae and

Gelencsér 2006; Weingartner et al. 2003). Consequently, brown carbon is also unlikely to play a strong role in the elevation of CN-to-HH σ_{ap}.

Additionally, there were no significant changes in relative humidity and temperature from the first to the second week as the average humidity and average temperature of the second week (average humidity and temperature of 62.57±6.02 % and 12.14±1.22 °C, respectively) were almost the same as those of the first week (62.33±6.47 % and 13.17±1.60 °C, respectively) (Fig. 1b). As a result, humidity and temperature are not expected to have a significant impact on σ_{ap} (Redemann et al. 2001; Mikhailov et al. 2006).

To sum up, among a number of factors that might contribute to the changes of σ_{ap}, HH caused increase in internal mixing is solely confirmed in this study.

In situ light absorption measurements needed

Although the enhancement of the σ_{ap} value for EC (and consequently the measured BC) during HH conditions has been argued, the exact enhancement that took place in our study is unavailable because our monitoring scheme could only obtain the filter-based ATN, rather than in situ absorption, b_{ap}. Considering that total ATN incorporates not only b_{ap} but also filter-induced light attenuation (mainly light scattering due to the filter matrix and the particles embedded in the filter matrix) (Arnott et al. 2005; Petzold et al. 1997; Weingartner et al. 2003; Chow et al. 2009), the abovementioned BC/EC ratios of 1.88±0.30 for the HH week and 0.92 ±0.14 for the CN week can suggest an enhancement factor of approximately two for the attenuation efficiency, σ_{ATN-a}, but not for σ_{ap}.

However, the enhancement factor of σ_{ap} for airborne aerosol EC from CN to HH conditions is important for characterizing trends in the regional climate, visibility, and atmospheric chemistry; consequently, future research initiatives should include a monitoring program to measure b_{ap} for CN and HH conditions. Two methods can be used to obtain b_{ap}. For the first method, a nephelometer can be used to monitor aerosol scattering (b_{scat}) simultaneously with an aethalometer to monitor ATN; b_{ap} can then be calculated using a correction procedure (Arnott et al. 2005; Coen et al. 2010; Schmid et al. 2006; Weingartner et al. 2003). In the second approach, b_{ap} can be monitored directly using non-filter-based instruments. For example, a photoacoustic analyzer (PA) measures b_{ap} directly by detecting the acoustic signal

produced when the sample stream is heated due to the absorption of laser light by airborne particles (Arnott et al. 1999; Japar et al. 1982). The PA has been considered to be a fundamental standard for b_{ap}, provided that appropriate calibration and baseline corrections for the absorption by gases are performed (Arnott et al. 2000).

Implication for the possibility of EC as an indicator

First, research is recommended on using EC as an indicator of anthropogenic interference in the atmospheric environment. The emission of EC into the atmosphere results from the incomplete combustion of carbon-containing substances; the removal of EC from the atmosphere depends only on natural deposition. That is, no other processes in the atmosphere introduce EC or chemically transform EC into another substance (secondary aerosols, for example) (Turpin and Huntzicker 1995). This characteristic makes EC one of the rare atmospheric components that maintain a clear lifelong identity as a primary air pollutant; therefore, EC may offer a potential indicator of direct anthropogenic interference in the atmospheric environment through energy consumption, such as power generation by coal, residential cooking/heating, and motorized vehicles fueled by diesel or petroleum. This suggestion is indirectly corroborated by the decline in the EC/$PM_{2.5}$ ratio from 0.074±0.021 during the CN week to 0.046±0.006 during the HH week (According to Table 1), which was presumably due to the increased formation of secondary particles (non-EC) when the weather changed from CN to HH (Fig. 5), indicating the unique role of EC to reflect the actual primary emissions related to human activities. Another example was reported by Keuken et al. (2012); in their study, they recommended EC as an indicator for evaluating the impact of traffic measures on air quality and health.

In addition, research is also recommended on using EC as an indicator of natural magnification of direct anthropogenic pollution. As described above, σ_{ap} depends much on the degree of internal mixing of EC with other species, including secondary species; the stagnant weather conditions that led to HH entailed enhanced internal mixing and therefore an increased σ_{ap}.

We acknowledge that the experimental duration of only 2 weeks, including 1 week for CN and 1 week for HH in this study, is short; a longer observation period, such as one that extends for a full year, is needed to study the EC/BC relationship and the relevant optical properties in full response to the effects of HH. Despite this limitation and although the exact σ_{ap} enhancement factor was not fully ascertained in this study, the HH-induced increases in both the measured EC, BC/EC ratio, OC/EC ratio, and σ_{ap} have been unambiguously validated not only in this study but also in other research, (e.g., Yang et al. 2011; Tan et al. 2009), which is extremely informative and therefore worthy of further study. Given these results, we suggest a systematic probe into the inclusion of the EC complex (EC concentration, OC/EC ratio, and σ_{ap}) as an indicator in air quality observations, alert systems for the evaluation of air quality, and the governance of emissions and human behaviors.

Conclusion

We conducted a specific monitoring of the EC/BC relationship during the transition from normal air quality to heavy haze. We observed that BC/EC ratio during the HH period doubled that during the CN period, which is confirmed to result partially from an increase in the in situ light absorption efficiency (σ_{ap}) due to the enhanced internal mixing of the EC with other species, though the exact enhancement factor was unresolved here. This reveals a need to investigate the exact enhancement by measurement of the EC value and in situ b_{ap} under both CN and HH conditions. Moreover, given the EC performance linked to both anthropogenic emissions and air quality, we advocate a systematic study on how to use *EC complex* (EC concentration, OC/EC ratio, and σ_{ap}) as an indicator in air quality observations, in alert systems, and in the governance of emissions and human behaviors.

References

Allen, R. J., Sherwood, S. C., Norris, J. R., & Zender, C. S. (2012). Recent northern hemisphere tropical expansion primarily driven by black carbon and tropospheric ozone. *Nature, 485*, 350–354.

Andreae, M. O., & Gelencsér, A. (2006). Black carbon or brown carbon? The nature of light-absorbing carbonaceous aerosols. *Atmospheric Chemistry and Physics, 6*, 3131–3148.

Arnott, W. P., Moosmuller, H., Rogers, C. F., Jin, T., & Bruch, R. (1999). Photoacoustic spectrometer for measuring light absorption by aerosol: instrument description. *Atmospheric Environment, 33*(17), 2845–2852.

Arnott, W. P., Moosmüller, H., & Walker, J. W. (2000). Nitrogen dioxide and kerosene-flame soot calibration of photoacoustic instruments for measurement of light absorption by aerosols. *Review of Scientific Instruments, 71*, 4545–4552.

Arnott, W. P., Hamasha, K., Moosmuller, H., Sheridan, P. J., & Ogren, J. A. (2005). Towards aerosol light-absorption measurements with a 7-wavelength aethalometer: evaluation with a photoacoustic instrument and 3-wavelength nephelometer. *Aerosol Science & Technology, 39*(1), 17–29.

Birch, M. E. (1998). Analysis of carbonaceous aerosols: interlaboratory comparison. *Analyst, 123*(5), 851–857.

Birch, M. E. (2002). Occupational monitoring of particulate diesel exhaust by NIOSH method 5040. *Applied Occupational and Environmental Hygiene, 17*(6), 400–405.

Birch, M. E., & Cary, R. A. (1996). Elemental carbon-based method for occupational monitoring of particulate diesel exhaust: methodology and exposure issues. *Analyst, 121*, 1183–1190.

Biswas, S. K., Tarafdar, S. A., Islam, A., Khaliquzzaman, M., Tervahattu, H., & Kupiainen, K. (2003). Impact of unleaded gasoline introduction on the concentration of lead in the air of Dhaka, Bangladesh. *Journal of Air & Waste Management Association, 53*, 1355–1362.

Bond, T. C., & Bergstrom, R. W. (2006). Light absorption by carbonaceous particles: an investigative review. *Aerosol Science and Technology, 40*, 27–67.

Bond, T. C., Doherty, S. J., Fahey, D. W., Forster, P. M., Berntsen, T., DeAngelo, B. J., et al. (2013). Bounding the role of black carbon in the climate system: a scientific assessment. *Journal of Geophysical Research*. doi:10.1002/jgrd.50171.

Castro, L. M., Pio, C. A., Harrison, R. M., & Smith, D. J. T. (1999). Carbonaceous aerosol in urban and rural European atmospheres: estimation of secondary organic carbon concentrations. *Atmospheric Environment, 33*, 2771–2781.

Chang, D., Song, Y., & Liu, L. (2009). Visibility trends in six megacities in China 1973–2007. *Atmospheric Environment, 94*(2), 161–167.

Che, H., Zhang, X., Li, Y., Zhou, Z., & Qu, J. J. (2007). Horizontal visibility trends in China 1981–2005. *Geophysical Research letters, 34*, L24706. doi:10.1029/2007GL031450.

Chow, J. C., Watson, J. G., Pritchett, L. C., Pierson, W. R., Frazier, C. A., & Purcell, R. G. (1993). The DRI thermal/optical reflectance carbon analysis system: description, evaluation and applications in U.S. air quality studies. *Atmospheric Environment, 27A*(8), 1185–1201.

Chow, J. C., Watson, J. G., Chen, L. W., Chang, M. C., Robinson, N. F., Trimble, D., et al. (2007). The IMPROVE_A temperature protocol for thermal/optical carbon analysis: maintaining consistency with a long-term database. *Journal of Air & Waste Management Association, 57*(9), 1014–1023.

Chow, J. C., Watson, J. G., Doraiswamy, P., Chen, L.-W. A., Sodeman, D. A., Lowenthal, D. H., et al. (2009). Aerosol light absorption, black carbon, and elemental carbon at the Fresno Supersite, California. *Atmopheric Research, 93*(4), 874–887.

Coen, M. C., Weingartner, E., Apituley, A., Ceburnis, D., Flentje, H., Henzing, J. S., et al. (2010). Minimizing light absorption measurement artifacts of the aethalometer: evaluation of five correction algorithms. *Atmospheric Measurement Techniques, 3*, 457–474.

Conny, J. M., Klinedinst, D. B., Wight, S. A., & Paulsen, J. L. (2003). Optimizing thermal-optical methods for measuring atmospheric elemental (black) carbon: a response surface study. *Aerosol Science & Technology, 37*, 703–723.

Cyrys, J., Heinrich, J., Hoek, G., Meliefste, K., Lewne, M., Gehring, U., et al. (2003). Comparison between different traffic-related particle indicators: elemental carbon (EC), PM$_{2.5}$ mass, and absorbance. *Journal of Exposure Analysis and Environmental Epidemiology, 13*, 134–143.

Deng, X., Tie, X., Wu, D., Zhou, X., Bi, X., Tan, H., et al. (2008). Long-term trend of visibility and its characterizations in the Pearl River Delta (PRD) region, China. *Atmospheric Environment, 42*, 1424–1435.

Engling, G., & Gelencsér, A. (2010). Atmospheric particles: from local air pollution to climate change. *Elements, 6*(4), 223–222.

Feng, Y., Chen, Y., Guo, H., Zhi, G., Xiong, S., Li, J., et al. (2009). Characteristics of organic and elemental carbon in PM$_{2.5}$ samples in Shanghai, China. *Atmospheric Research, 92*(4), 434–442.

Gray, H. A., & Cass, G. R. (1998). Source contributions to atmospheric fine carbon particle concentrations. *Atmospheric Environment, 32*, 3805–3825.

Hansen, A. D. A., Rosen, H., & Novakov, T. (1984). The aethalometer—an instrument for the realtime measurement of optical absorption by aerosol particles. *Science of Total Environment, 36*, 191–196.

Huntzicker, J. J., Johnson, R. L., Shah, J. J., & Cary, R. A. (1982). *Analysis of organic and elemental carbon in ambient aerosols by the thermal-optical method* (Particulate carbon: atmospheric life cycle). New York: Plenum Press.

Jacobson, M. Z. (2000). A physically-based treatment of elemental carbon optics: implications for global direct forcing of aerosols. *Geophysical Research Letters, 27*, 217–220. doi:10.1029/1999GL010968.

Jacobson, M. Z. (2001). Strong radiative heating due to the mixing state of black carbon in atmospheric aerosols. *Nature, 409*, 695–697.

Japar, S. M., Moore, J., Killinger, D. K., & Szkarlat, A. C. (1982). Spectrophone measurements of diesel vehicle particulate material. In H. E. Gerber & E. E. Hindman (Eds.), *Light absorption by aerosol particles* (pp. 275–278). Hampton: Spectrum Press.

Jeong, C. H., Hopke, P. K., Kim, E., & Lee, D. W. (2004). The comparison between thermal-optical transmittance elemental carbon and aethalometer black carbon measured at multiple monitoring sites. *Atmospheric Environment, 38*, 5193–5204.

Johnson, R. L., & Huntzicker, J. J. (1979). Analysis of volatilizable and elemental carbon in ambient aerosols. In T. Novakov (Ed.), *Carbonaceous particles in the atmosphere* (pp. 10–13). Berkeley: Lawrence Berkeley Laboratory.

Kaul, D. S., Gupta, T., Tripathi, S. N., Tare, V., & Collett, J. L. (2011). Secondary organic aerosol: a comparison between foggy and nonfoggy days. *Environmental Science & Technology, 45*(17), 7307–7313.

Keuken, M. P., Jonkers, S., Zandveld, P., Voogt, M., & van den Elshout, S. (2012). Elemental carbon as an indicator for evaluating the impact of traffic measures on air quality and health. *Atmospheric Environment, 51*, 1–8.

Lavanchy, V. M. H., Gäggeler, H. W., Nyeki, S., & Baltensperger, U. (1999). Elemental carbon (EC) and black carbon (BC) measurements with a thermal method and an aethalometer at the highalpine research station Jungfraujoch. *Atmospheric Environment, 33*(17), 2759–2769.

Li, Y., Zhang, X., Gong, S., Che, H., Wang, D., Qu, W., et al. (2006). Comparison of EC and BC and evaluation of dust aerosol contribution to light absorption in Xi'an, China. *Environmental Monitoring and Assessment, 120*, 301–312.

Liu, D. Y., Wenzel, R. J., & Prather, K. A. (2003). Aerosol time-of-flight mass spectrometry during the Atlanta supersite experiment: 1. Measurements. *Journal of Geophysical Research, 108.* doi:10.1029/2001JD001562.

Mikhailov, E. F., Vlasenko, S. S., Podgorny, I. A., Ramanathan, V., & Corrigan, C. E. (2006). Optical properties of soot-water drop agglomerates: an experimental study. *Journal of Geophysical Research, 111.* doi:10.1029/2005JD006389.

Molnar, A., Meszaros, E., Hasson, H. C., Karlsson, G. A., Kiss, G. Y., & Krivacsy, Z. (1999). The importance of organic and elemental carbon in the fine atmospheric aerosol particles. *Atmospheric Environment, 33*, 2745–2750.

Nordmann, S., Birmili, W., Weinhold, K., Wiedensohler, A., Mertes, S., Müller, K., et al. (2009). Atmospheric aerosol measurements in the German Ultrafine Aerosol Network (GUAN), Part 2: comparison of measurements techniques for graphitic, lightabsorbing, and elemental carbon, and non-volatile particle volume under field conditions. *Gefahrstoffe-Reinhaltung der Luft, 69*, 469–474.

Pavuluri, C. M., Kawamura, K., Aggarwal, S. G., & Swaminathan, T. (2011). Characteristics, seasonality and sources of carbonaceous and ionic components in the tropical Indian aerosols. *Atmospheric Chemistry and Physics, 11*, 3937–3976.

Petzold, A., Kopp, C., & Niessner, R. (1997). The dependence of the specific attenuation cross-section on black carbon mass fraction and particle size. *Atmospheric Environment, 31*, 661–672.

Ramanathan, V., & Carmichael, G. (2008). Global and regional climate changes due to black carbon. *Nature Geoscience, 1*, 221–227.

Ramanathan, V., & Feng, Y. (2009). Air pollution, greenhouse gases and climate change: global and regional perspectives. *Atmospheric Environment, 43*, 37–50.

Redemann, J., Russell, P. B., & Hamill, P. (2001). Dependence of aerosol light absorption and single-scattering albedo on ambient relative humidity for sulfate aerosols with black carbon cores. *Journal of Geophysical Research, 106*, 27485–27495.

Salako, G. O., Hopke, P. K., Cohen, D. D., Begum, B. A., Biswas, S. K., Pandit, G. G., et al. (2012). Exploring the variation between EC and BC in a variety of locations. *Aerosol and Air Quality Research, 12*, 1–7.

Schmid, O., Artaxo, P., Arnott, W. P., Chand, D., Gatti, L. V., Frank, G. P., et al. (2006). Spectral light absorption by ambient aerosols influenced by biomass burning in the Amazon Basin. I: comparison and field calibration of absorption measurement techniques. *Atmospheric Chemistry and Physics, 6*, 3443–3462.

Seinfeld, J. H., & Pandis, S. N. (1998). *Atmospheric chemistry and physics: from air pollution to climate change*. New York: Wiley.

Stone, A. E., Schauer, J. J., Pradhan, B. B., Dangol, M. P., Habib, G., Venkataraman, C., et al. (2010). Characterization of

emissions from South Asian biofuels and application to source apportionment of carbonaceous aerosol in the Himalayas. *Journal of Geophysical Research, 115*, 1–14.

Sun, Y., Zhuang, G., Tang, A., Wang, Y., & An, Z. (2006). Chemical characteristics of $PM_{2.5}$ and PM_{10} in haze-fog episodes in Beijing. *Environmental Science & Technology, 40*(10), 3148–2155.

Tan, J., Duan, J., He, K., Ma, Y., Duan, F., Chen, Y., et al. (2009). Chemical characteristics of $PM_{2.5}$ during a typical haze episode in Guangzhou. *Journal of Environmental Sciences, 21*, 774–781.

Turco, R. P., Toon, O. B., Whitten, R. C., Pollack, J. B., & Hamill, P. (1983). The global cycle of particulate elemental carbon: a theoretical assessment. In H. R. Pruppacher (Ed.), *Precipitation scavanging, dry deposition, and resuspension* (pp. 1337–1351). New York: Elsevier Sci.

Turpin, B. J., & Huntzicker, J. J. (1995). Identification of secondary aerosol episodes and quantitation of primary and secondary organic aerosol concentrations during SCAQS. *Atmospheric Environment, 29*, 3527–3544.

Turpin, B. J., Huntzicker, J. J., & Amams, K. M. (1990). Intercomparison of photoacoustic and thermal-optical methods for the measurement of atmospheric elemental carbon. *Atmopheric Environment, Part A. General Topics, 24*(7), 1831–1835.

Vignati, E., Karl, M., Krol, M., Wilson, J., Stier, P., & Cavalli, F. (2010). Sources of uncertainties in modelling black carbon at the global scale. *Atmospheric Chemistry and Physics, 10*, 2595–2611.

Watson, J. G., Chow, J. C., & Chen, L.-W. (2005). Summary of organic and elemental carbon/black carbon analysis methods and intercomparisons. *Aerosol and Air Quality Research, 5*(1), 65–102.

Weingartner, E., Saathoff, H., Schnaiter, M., Streit, N., Bitnar, B., & Baltensperger, U. (2003). Absorption of light by soot particles: determination of the absorption coefficient by means of aethalometers. *Journal of Aerosol Science, 34*(10), 1445–1463.

Wolff, G. T. (1981). Particulate elemental carbon in the atmosphere. *Journal of the Air Pollution Control Association, 31*, 935–939.

Wu, D., Tie, X., Li, C., Ying, Z., Lau, A. K.-H., Huang, J., et al. (2005). An extremely low visibility event over the Guangzhou region: a case study. *Atmospheric Environment, 39*(35), 6568–6577.

Yang, F., Chen, H., Du, J., Yang, X., Gao, S., Chen, J., et al. (2011). Evolution of the mixing state of fine aerosols during haze events in Shanghai. *Atmospheric Research, 104–105*, 193–201.

Zhi, G., Chen, Y., Feng, Y., Xiong, S., Li, J., Zhang, G., et al. (2008). Emission characteristics of carbonaceous particles from various residential coal-stoves in China. *Environmental Science & Technology, 42*(9), 3310–3315.

Zhi, G., Peng, C., Chen, Y., Liu, D., Sheng, G., & Fu, J. (2009). Deployment of coal-briquettes and improved stoves: possibly an option for both environment and climate. *Environmental Science & Technology, 43*(15), 5586–5591.

Zhi, G., Chen, Y., Sun, J., Chen, L., Tian, W., Duan, J., et al. (2011). Harmonizing aerosol carbon measurements between two conventional thermal/optical analysis methods. *Environmental Science & Technology, 45*(7), 2902–2908.